LA-UR-19-22723
Approved for public release; distribution is unlimited.

Title: Hydrogen Transport in a Model 9979 Shipping Package with Inner Convenience Cans

Author(s): Coons, James Elmer
Martinez, Patrick Thomas
French, Sean B.
Morley, Richard Alfred

Intended for: Report

Issued: 2020-02-26 (rev.2)

Hydrogen Transport in a Model 9979 Shipping Package with Inner Convenience Cans

by

J. E. Coons[1], P. T. Martinez[2], S. B. French[2], and R. A. Morley[2]

[1]Chemical Diagnostics and Engineering Group
[2]Actinide Analytical Chemistry Group
Chemistry Division
Los Alamos National Laboratory
P.O. Box 1663
Los Alamos, NM 87545

April 10, 2019

Ver 1.1

LA-UR-19-22723

TABLE OF CONTENTS

Executive Summary

Radiolytic hydrogen production and accumulation inside containment packages is a concern at any facility responsible for their packaging, storage, transportation, and/or disposal. When hydrogen gas accumulates to concentrations above the Lower Flammability Limit (LFL) which is 4% or 40,000 ppm in air, the possibility of a deflagration or explosion increases. This concern persists over the course of the package lifetime which is unlimited when disposed of by burial or in permanent repositories. Here, we report on a numerical model used to predict the concentration of hydrogen within each layer of a Model 9979 package containing a convenience can assembly. Simulations show the hydrogen concentration to always be highest in the inner convenience can containing the radioactive source. When the radioactive source is within the Los Alamos National Laboratory (LANL) Packaging Limits, the hydrogen concentration is shown to remain well below the LFL at all times including packaging, storage, transportation, and disposal.

A hydrogen transport model is presented for a Model 9979 package system containing a nested arrangement of convenience cans, which are tin oxide coated steel cans of various sizes with a slip-lid assembly. The inner convenience can contains the radioactive source material along with an unknown quantity of incidental water acquired from humid air or processing. While visible organic materials such as paper and plastics were purposely excluded from the inner can, it is not possible to claim the wastes are entirely organic free. The inner convenience can is tape sealed and placed into a plastic bag which is horsetail closed (i.e., twisted and taped). The bagged can is placed into an outer convenience can that is also tape sealed. The can assembly is then placed into the 30 gallon drum and subsequently placed inside the 55 gallon drum in the 9979 package. Here we assume hydrogen gas is produced in the inner convenience can from alpha radiolysis of water at a rate dependent on the quantity of uranium isotopes and water present. The hydrogen transport model was used to calculate hydrogen accumulations within the package's five layers at different times and conditions. These simulations serve two purposes; (i) to build confidence in the model by comparing predicted values to measured values, and (ii) to check the steady state hydrogen concentrations that are approached at long times in the package's lifetime. Model simulations were compared to gas samples taken from the 30 gallon drum after storage at LANL's Chemistry and Metallurgy Research (CMR) building for around 500 days. Hydrogen concentration calculations over much longer periods (i.e., more than 270 years) included extreme storage durations, transportation at extreme cold temperatures, and disposal of packages assuming different average temperatures.

Maximum hydrogen concentrations obtained from hydrogen transport model simulations were compared to measured values from 5 packages. Gas samples were collected from the 30 gallon drum layer after approximately 500 days of storage at the CMR building. Calculated hydrogen gas concentrations were shown to bound the measured values in 4 of 5 packages. The hydrogen concentration in the one outlier package (i.e., 4033Drum#16) is about 48% higher than the predicted value, and likely results from organic material in the inner can as evinced by the detection of methane. Bounding of the measured hydrogen concentrations suggests the

parameter values used in the model are reasonable for the purpose of estimating maximum hydrogen gas accumulation in the 9979 package to within 50%. Hydrogen content calculated for the inner convenience can in all 5 packages is well below the hydrogen LFL value. A sensitivity analysis was performed on the model parameters around the assumed values, and it was concluded the only parameter that could account for the dramatically low hydrogen content in three of the five packages is the hydrogen generation rate efficiency factor. This reinforces the concept of applying an efficiency factor of 1 for conservative estimates of hydrogen content in the 9979 package.

The transport model was also used to calculate maximum hydrogen concentrations in various lifetime scenarios whereby packages were subjected to extreme storage, transportation, and disposal conditions. A storage period of 1200 days was applied, which is a longer than the maximum expected. A two week transportation period was assumed at extremely cold temperatures that severely reduce the transport of hydrogen out of the package. And finally, different average temperatures were assumed for disposal of the packages. The conditions of any given package are unique as a consequence of the amount of radioactive materials contained as well as its thermal and site history. Two extreme radioactive material limits were considered for the sake of identifying credible worst case hydrogen accumulation in the inner can.

1. LANL Criticality Limit: 1.5 g of U-234, 200 g of U-235, and 4900 g of U-238.
2. LANL Packaging Limit: 2.7 g of U-234, 350 g of U-235, and 8647.3 g of U-238.

The LANL Criticality Limit is a very conservative limit and contains roughly half the radioactive material as is in the LANL Package Limit. The hydrogen concentration is always highest in the inner convenience can and was calculated over periods exceeding 270 years where steady state values are approached. Simulations consisted of the following three distinct segments.

1. **Assembly and storage.** Assembly of the 9979 package was assumed to occur at LANL's CMR building, where it is stored for 1200 days at 20°C and 582 torr.
2. **Transportation.** Following storage, the 9979 package is transported to the Nevada Test Site (NTS) over a 14 day period at one of two extreme temperature conditions; either -28.89°C (-20°F) or -40°C (-40°F). Neither temperature raised concerns with the hydrogen LFL due to the relatively short time period. Atmospheric pressure was assumed constant at 582 torr, the average for Los Alamos, NM. Atmospheric pressure would more realistically transition from 582 to 678 torr, the average atmospheric pressure for Beatty, NV. Increasing atmospheric temperature has two disproportionate counteracting effects. High pressure air would flow into the 9979 package and drive down hydrogen concentrations. At the same time, increasing package pressure would reduce hydrogen diffusivity resulting in slightly more hydrogen accumulation. Even though the dilution effect is estimated to be larger than the net gain in hydrogen due to reduced diffusivity, assuming continuity of pressure and hydrogen concentrations through the transport period simplifies the calculations and provides more conservative estimates of hydrogen concentration throughout the 9979 package.

3. **Final disposition (burial).** Burial of the 9979 package was assumed to occur at Beatty, NV, where the average atmospheric pressure is 678 torr. Three temperatures were considered for this final lifetime segment; the average low temperature of 6.1°C, the average temperature of 14.75°C, and the average high temperature of 23.4°C. While it is likely the initial hydrogen concentrations in a 9979 package would be slightly reduced following pressurization in the Beatty atmosphere, the hydrogen concentrations calculated at the end of the transportation period were taken without change as the initial values for the final disposition period. Maintaining continuity of hydrogen concentrations between the transportation and disposition segments is consistent with the desire to provide conservative estimates of hydrogen concentration in the 9979 package.

Lifetime simulations of the hydrogen concentration in the inside can indicate steady state conditions are reached after several decades and at no time encroach on the hydrogen LFL. Solutions at long times (i.e., around 100,000 days) obtained with the dynamic model were found to be in agreement with the steady state values. Therefore, this analysis shows that 9979 drums packaged at LANL will never exceed nor closely approach the hydrogen LFL needed for a deflagration or fire event. Extended storage at LANL, extremely cold transportation temperatures, or burial at Beatty, NV will not alter the safe levels of hydrogen in the container system even over extremely long times.

Introduction

Radiolytic hydrogen production and accumulation in containment packages is of general concern at facilities responsible for their packaging, storage, transportation, and/or disposal. When hydrogen gas accumulates to concentrations above the Lower Flammability Limit (LFL)[1] which is 4% or 40,000 ppm in air, the possibility of a deflagration or explosion increases. This concern persists over the course of the package lifetime which is unlimited when disposed of by burial or in permanent repositories. Here, we report on a numerical model used to predict the concentration of hydrogen within each layer of a Model 9979 package containing a convenience can assembly. Container scenarios with uranium contents equivalent to LANL Criticality and Packaging Limits are modeled following packaging and storage for 1200 days at Los Alamos National Laboratory (LANL), shipment at extreme cold conditions (-28.89 and -40°C), and permanent burial at the Nevada Test Site (NTS) in Beatty, NV. In all scenarios, the hydrogen concentration is highest in the inner convenience can containing the radioactive source material. When the radioactive source is within the LANL Packaging Limits, the hydrogen concentration is shown to remain well below the LFL at all times throughout packaging, storage, transportation, and disposal.

Nomenclature

The following nomenclature and units were employed for the derivation of model equations.

A	Membrane or material surface area or area normal to gaseous diffusion (cm^2).
$C_{H_2,i}$	concentration of hydrogen gas in the i^{th} layer ($moles/cm^3$).
D	Diffusion coefficient of hydrogen atoms through steel (cm^2/day).
D_{AB}	Molecular diffusivity of gas A in gas B, or vice versa (cm^2/day).
$D_{eff,i}$	Effective diffusion coefficient of hydrogen gas through the barrier separating the i^{th} layer and the $(i+1)^{th}$ layer (moles/day/mole fraction).
d	Can or container diameter, (cm).
$\dot{g}_{H_2}$	Hydrogen gas production rate (moles/day).
h	Membrane or material height (cm).
$K_{0,i}$	Membrane permeation coefficient (moles/cm/day/torr).
k	Boltzmann's constant, 1.381×10^{-23} (Nm/°K).
$k_{eff,PG}$	Rate constant for purge gas in air diffusion determined experimentally (day^{-1}).
L	Membrane or material thickness (cm).
M_A	Molecular weight of species A (g/mole).
m_0	Mass of the taped can when filled with purge gas (e.g., helium) (g).
$m(t)$	Mass of the taped can at time t (g).
m_∞	Mass of the taped can when filled with air (g).

[1] National Fire Protection Association, NFPA 497, *Recommended Practice for the Classification of Flammable Liquids, Gases, or Vapors and of Hazardous (Classified) Locations for Electrical Installations in Chemical Process Areas*, 2017.

N Molar flux of gas (moles/cm^2/day).
$n_{Tot,i}$ moles of gas in the ith layer (moles).
P Atmospheric pressure at the package location (torr).
Q Hydrogen transport rate (moles/day).
Q_{Comp} Hydrogen transport rate through the steel/polyurethane composite in the 55 gallon drum (moles/day).
Q_{EPDM} Hydrogen transport rate through the EPDM gasket (moles/day).
Q_{PU} Hydrogen transport rate through the polyurethane foam support in the 55 gallon drum (moles/day).
Q_{Si} Hydrogen transport rate through the silicone gasket (moles/day).
Q_{SnO_2} Hydrogen transport rate through tin oxide coated can walls (moles/day/$\sqrt{\text{torr}}$).
$Q_{Steel30}$ Hydrogen transport rate through steel walls in the 30 gallon drum (moles/day/$\sqrt{\text{torr}}$).
$Q_{Steel55}$ Hydrogen transport rate through steel walls in the 55 gallon drum (moles/day/$\sqrt{\text{torr}}$).
R Ideal gas constant (62363.67 cc torr/gmole /°K).
r_{A} Molecular separation at collision of species A (Å).
r_{AB} Molecular separation at collision of species A with species B (Å).
S_i Hydrogen solubility in the ith layer (moles/cc material).
S_0 Hydrogen solubility (moles/cc material/$\sqrt{\text{torr}}$).
T Temperature at the facility location (°K).
t Time (days).
V_{can} Void volume of the can in the purge gas experiments (cm^3).
V_i Void volume of the the ith layer (cm^3).
y_i Mole fraction of hydrogen gas in the void volume of the *ith* layer (dimensionless).
z Diffusion path length across the can gap (cm).

Greek

ε_{A}/k Energy of molecular attraction between molecules of species A (°K).
$\varepsilon_{\text{AB}}/k$ Energy of molecular attraction between molecules of species A and species B (°K).
η Hydrogen generation rate efficiency factor, $\eta \leq 1$ (dimensionless).
$\phi_{SnO_2,i}$ Hydrogen permeability through the tin oxide barrier of the slip lid can in the ith layer (moles cm/cm^2/day/$\sqrt{\text{torr}}$).
Ω_D Diffusion collision integral (dimensionless).

System description

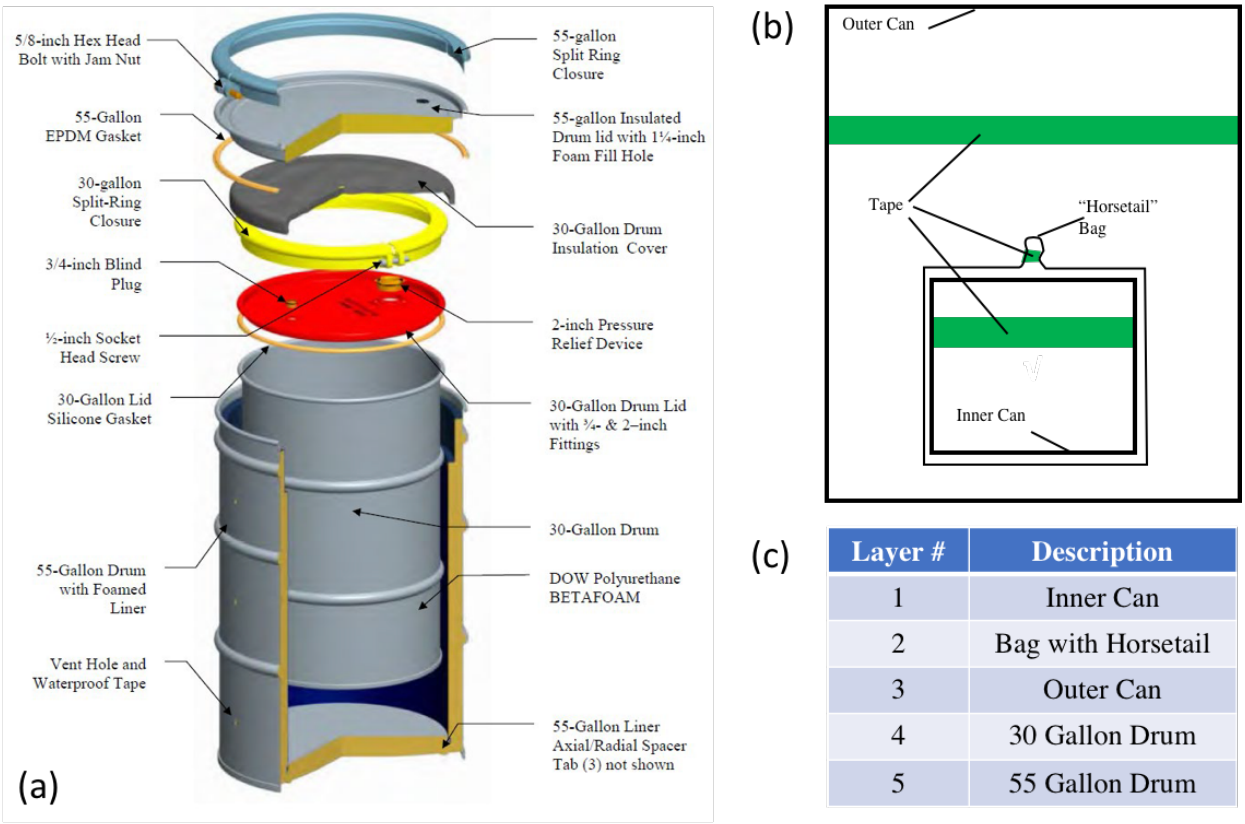

(c)

Layer #	Description
1	Inner Can
2	Bag with Horsetail
3	Outer Can
4	30 Gallon Drum
5	55 Gallon Drum

Figure 1. Model 9979 Type AF shipping package (a) with inner can assembly (b) assumed in the transport model. The layer description used in the model is also shown in the associated table (c).

The containment system applied in the transport model consists of a taped convenience can placed within the 30 gallon drum of the Model 9979 Type AF Shipping Container[2] shown in Figure 1(a). The taped convenience can is called the outer can (see Figure 1(b) and (c)), and the contents of the outer can are prepared starting with the inner can. All radioactive source materials are placed inside the inner can, followed by placement of the inner can's slip-top lid. Radioactive uranium, decay compounds of uranium, and other inorganic materials including water are contained within the inner can. Organic materials are assumed to be excluded from the inner can volume. Once the inner can is lidded, the lid position is secured by tape as shown in Figure 1(b). The lidded and taped inner can is wrapped tightly in a plastic bag by twisting and taping the bag to effect a horsetail closure. The bagged inner can is then placed within the outer can, which is lidded and tape secured as with the inner can. The outer can is then placed within the 30 gallon drum and the lid secured with a silicone gasket in place. The 30 gallon drum is placed in the 55 gallon drum, which is closed following installation of the 30 gallon drum cover and closure of the 55 gallon drum lid is secured with the EPDM seal in place. Both

[2] French, S. B., Hydrogen Gas Concentration in Model 9979 Type AF Containers at Los Alamos National Laboratory, LA-UR-18-29921, October 2018.

drums are made of carbon steel and both inner and outer cans are made of carbon steel with a SnO_2 coating.

Effective Hydrogen Diffusivity

Figure 2. Taped cannister (Can 1) used for the helium and argon transport experiments. Can 2 was similarly constructed and assembled.

Given the hazards associated with high concentrations of hydrogen gas, effective hydrogen diffusivity values were estimated from transport experiments on two replicate convenience cans purged with helium and argon in separate experiments. As shown in Figure 2, a 2.2 liter tin-plated steel convenience can was used to represent the packaging placed into the 9979 Drums. Inlet and outlet valves were installed and epoxy sealed to the can's slip-top lid, allowing purging of the can with helium or argon gases. Experiments were conducted by P. Martinez (C-AAC) to measure the displacement of purge gas by air. The slip-top lid with valves was placed on the can and sealed with vinyl tape as in standard practice. The valves were closed following assembly and the mass of the air-filled can measured (m_∞). The tape-sealed can with then purged with either helium or argon and the valves closed. The mass of the can was measured immediately (m_0) and then periodically over several weeks $\big(m(t)\big)$. A Gow-Mac Model 21-070 Mini Gas Leak Detector was used to check the integrity of the valve lid seal following the purge, and no leak was detected.

In the displacement experiment, the can pressure is constant with time and the molar flux of the purge gas diffusing out of the container (N_{PG}) has to be equal (and opposite in sign) to the molar flux of air diffusing into the can (N_{Air}). This transport is described as steady-state equimolar counterdiffusion, which leads to the following expression for molar flux[3].

$$N_{PG} = -\frac{D_{PG,Air}(P/RT)}{z}\left(y_{PG,1} - y_{PG,Room}\right) \tag{1}$$

The left side of Eq. 1 can be replaced by the change in purge gas concentration within the can resulting from diffusion through the taped slip lid and can seams.

$$N_{PG} = \left(\frac{V_{can}}{A_{gap}}\right)\frac{dC_{PG,1}}{dt} = \frac{1}{A_{gap}}\left(\frac{PV_{can}}{RT}\right)\frac{dy_{PG,1}}{dt} \tag{2}$$

[3] Treybal, R. E., Mass-Transfer Operations, 3rd Edition, McGraw-Hill Book Company, 1980.

The right hand side of Eq. 1 can be simplified by assuming the room volume is infinitely large relative to that of the can, and therefore the mole fraction of purge gas in the room is always negligible $\left(y_{PG,Room} \approx 0\right)$. Combining Eq. 1 and 2 leads to the following expression.

$$\frac{dy_{PG,1}}{dt} = -\frac{D_{PG,Air}A_{gap}}{V_{can}z}\left(y_{PG,1}\right) = -k_{eff,PG}y_{PG,1} \tag{3}$$

$k_{eff,PG}$ is a rate constant capturing the equimolar diffusion in the experiment. Separating variables and integrating from $t = 0$ $(y_{PG} = 1)$ leads to the following characteristic equation.

$$y_{PG,1} = e^{-k_{eff,PG}t} \tag{4}$$

By assuming ideal gas conditions, it can be shown the mole fraction of purge gas at any given time can be calculated from the following normalized mass change.

$$y_{PG,1}(t) = \frac{m_\infty - m(t)}{m_\infty - m_0} \tag{5}$$

Therefore, the effective rate constant is obtained from the slope of the plot of the natural log of the normalized mass change with time. Experimental results from two convenience cans using helium and argon purge gases are shown in Figure 3, where rate constants 0.054 ± 0.002 day^{-1} and 0.070 ± 0.007 day^{-1} were obtained for helium and 0.018 ± 0.003 day^{-1} and 0.026 ± 0.007 day^{-1} were obtained for argon. Uncertainty in the rates was estimated as the standard deviation of rates calculated from each measured mole fraction.

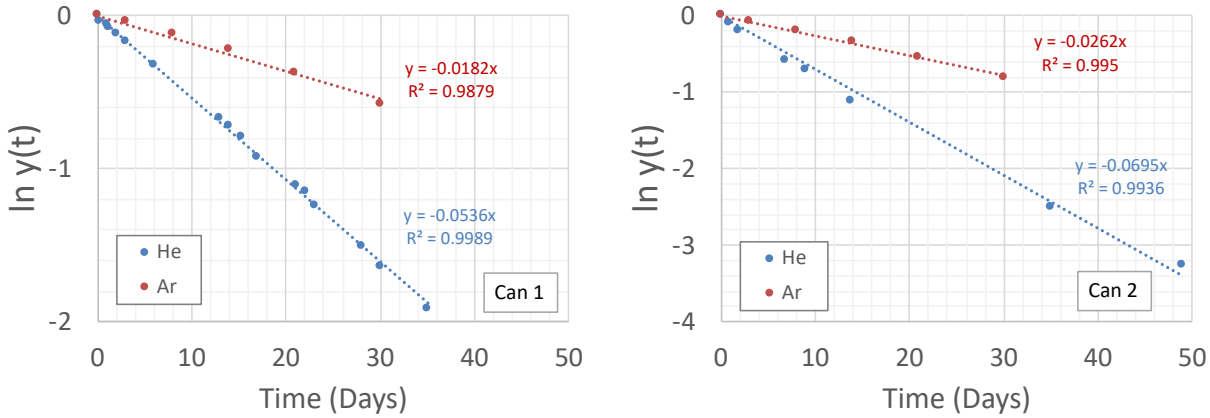

Figure 3. Effective rate constant measurements from helium and argon purge gas experiments in two cans. Data points are shown as symbols and linear fits are shown as dotted lines. The rates in Can 1 (left) are lower than in Can 2 (right), and are used to obtain conservative effective hydrogen diffusivity values for the hydrogen transport model.

Prior to using this result in the transport model, the effective rate constant has to be changed to the form of effective diffusivity $\left(D_{eff}\right)$ and also modified to take into account differences

resulting from hydrogen transport rather than helium and argon. Looking at Eq. 1, an explicit form of the effective diffusivity is obtained by multiplying the constant on the right hand side by the area normal to the gas flux (A_{gap}).

$$D_{eff,PG} = \frac{D_{PG,Air} A_{gap}}{z} \left(\frac{P}{RT}\right) \tag{6}$$

By comparing Eq. 6 to Eq. 3, the relationship between the effective diffusivity and rate constant becomes apparent.

$$D_{eff,PG} = k_{eff,PG} \left(\frac{PV_{can}}{RT}\right) \tag{7}$$

Taking the can volume as 2200 cm^3, the effective diffusivities at the laboratory temperature (20°C) and pressure (582 torr) are calculated to be 0.00375 ± 0.00014 and 0.0049 ± 0.0005 moles/day/mole fraction for helium, and 0.0013 ± 0.0002 and 0.0018 ± 0.0005 moles/day/mole fraction for argon. Eq. 6 shows the effective diffusivity to be directly proportional to the molecular diffusivity, which is expected to differ when hydrogen is the diffusing gas. Here we use Chapman-Enskog kinetic theory[4,5] to predict the molecular diffusivity of gases.

Under ideal gas conditions, the molecular diffusivity of gas A diffusing through gas B (or vice versa) is calculated from the following Chapman-Enskog[4,5] expression:

$$D_{AB} = \frac{1.22 \times 10^5 T^{1.5} \sqrt{1/M_A + 1/M_B}}{P r_{AB}^2 \Omega_D} \tag{8}$$

which is dependent on the characteristic length (r_{AB}), the energy of molecular attraction (ε_{AB}), and the diffusion collision integral (Ω_D) given by the following set of equations.

$$r_{AB} = (r_A + r_B)/2 \tag{9}$$

$$\varepsilon_{AB} = \sqrt{\varepsilon_A \varepsilon_B} \tag{10}$$

$$\Omega_D = \frac{1.06036}{(T^*)^{0.1561}} + \frac{0.193}{e^{(0.47635T^*)}} + \frac{1.03587}{e^{(1.52996T^*)}} + \frac{1.76474}{e^{(3.89411T^*)}} \tag{11}$$

$$T^* = kT/\varepsilon_{AB}. \tag{12}$$

[4] Bird, R. B., W. E. Stewart, and E. N. Lightfoot, Transport Phenomena, John Wiley & Sons, 1960.
[5] Reid, R. C., J. M. Prausnitz, and B. E. Poling, The Properties of Gases & Liquids, McGraw-Hill, Inc., 4th Edition, 1987.

The energy of molecular attraction (ε_A) and molecular separation at collision (r_A) for each gas was taken from Svehla[6], and are provided in Table 1 below for convenience.

Table 1. Species parameters used in Equations 9 and 10.

Molecular Species:	**Air**	**Ar**	**He**	**H_2**
$\boldsymbol{\varepsilon_A/k}$ **(°K)**	78.6	93.3	10.22	59.7
$\boldsymbol{r_A}$ **(Å)**	3.711	3.542	2.551	2.827

Relevant paired parameters are provided in Table 2.

Table 2. Paired parameters at laboratory temperature.

Gas Pair, *AB*	$\boldsymbol{\varepsilon_{AB}/k}$ **(°K)**	$\boldsymbol{r_{AB}}$ **(Å)**	$\boldsymbol{\Omega_D^{20°C}}$	$\boldsymbol{\frac{\sqrt{1/M_A + 1/M_B}}{r_{AB}^2 \Omega_D^{20°C}}}$
Ar, Air	85.6	3.627	0.918	0.0202
He, Air	28.3	3.131	0.738	0.0737
H_2, Air	68.5	3.269	0.872	0.0782

Substitution of Eq. 8 into Eq. 6 elucidates the fundamental dependencies of the effective diffusivity.

$$D_{eff,PG} \propto \frac{(T^{0.5}/\Omega_D)\sqrt{1/M_{Air} + 1/M_{PG}}}{r_{Air,PG}^2}\left(\frac{A_{gap}}{z}\right) \tag{13}$$

Note that the effective diffusivity has no pressure dependence and its temperature dependence ($T^{0.5}/\Omega_D$) is reduced relative to that of molecular diffusion ($T^{1.5}/\Omega_D$). At constant temperature, the effective diffusivity is a function of the paired parameters, the gap area and diffusion path length(z). Assuming the gap and path dimensions are fixed in each can, the constant temperature effective diffusivity becomes only a function of the paired parameters.

$$D_{eff,PG}\big|_T \propto \frac{\sqrt{1/M_{Air} + 1/M_{PG}}}{r_{Air,PG}^2 \Omega_D} \tag{14}$$

This relationship is tested in Figure 4 where the effective diffusivities measured in each can are plotted against the parameter on the right hand side of Eq. 14 (also provided in Table 2). The proportionality constant is shown to be about 24% smaller in Can 1. A conservative estimate of the effective diffusivity of hydrogen at room temperature was calculated from the product of

[6] Svehla, R. A., Estimated Viscosities and Thermal Conductivities of Gases at High Temperatures, National Aeronautics and Space Administration Technical Report R-132, 1962.

the Can 1 proportionality constant and the air-hydrogen paired parameters of Eq. 14 (provided in Table 2) as 0.00405 moles/day/mole fraction.

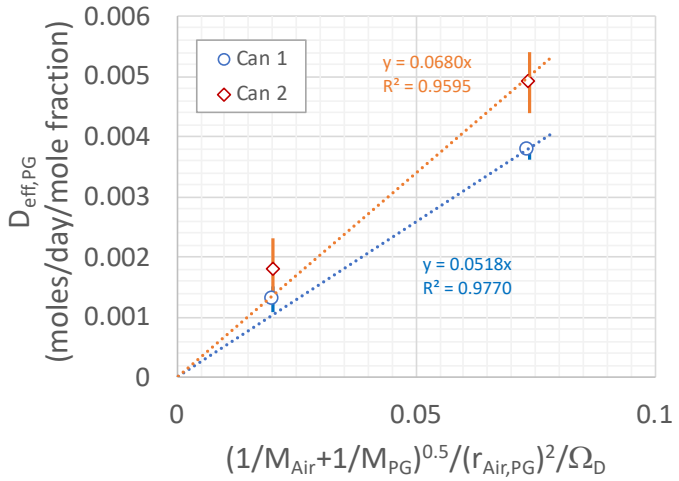

Figure 4. The effective diffusivities of argon and helium in air measured experimentally in each containment can plotted against the paired parameters of Eq. 14. Agreement of the data with Eq. 14 provides the basis for estimating the effective hydrogen diffusivity.

A general expression for the effective diffusivity of hydrogen in air for the container cans can be derived by exploring the temperature and can size dependencies. The effective diffusivity of hydrogen can be estimated at any temperature with the adjustment provided in Eq. (15).

$$D_{eff,H_2}\big|_T = \frac{(T^{0.5}/\Omega_D)|_T}{(T^{0.5}/\Omega_D)|_{20°C}} D_{eff,H_2}\big|_{20°C} \tag{15}$$

The effective diffusivity of hydrogen was calculated using Eq. 15 and the parameter values in Table 3 over the temperature range of interest. The results are plotted in Figure 5.

Table 3. Calculated effective diffusivity over the relevant temperature range.

T (°C)	$(T^{0.5}/\Omega_D)$	D_{eff,H_2} (moles/day/mole fraction)
-40	16.60	0.00342
-20	17.65	0.00364
20	19.64	0.00405
67.2	21.85	0.00451

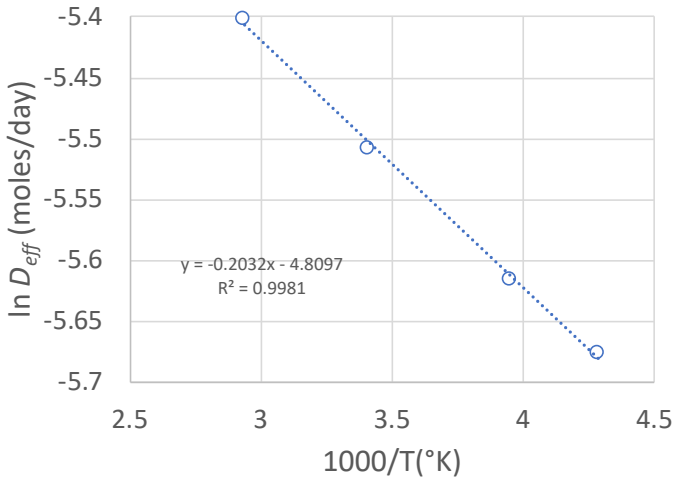

Figure 5. The effect of temperature on the effective diffusivity for hydrogen transport from the convenience can. Symbols correspond to calculated values listed in Table 3. The linear fit leads to Eq. 16.

While the effective diffusivities in Table 3 and Figure 5 were calculated assuming a fixed gap area and diffusion path length, the gap area would change if a different size can were to be used. More specifically, the gap area is assumed to be directly proportional to the can circumference. A generalized equation for the effective diffusivity for hydrogen transport from a taped convenience can is obtained by incorporating the diameter dependence into the exponential equation resulting from the linear fit of Figure 5, as shown in Eq. 16.

$$D_{eff,1} = 8.15 \times 10^{-3} \left(\frac{d_1}{15\ \text{cm}}\right) exp^{\left(\frac{-203.2}{T}\right)} \tag{16}$$

Model Formulation

The hydrogen gas content in each layer volume in the 9979 container system is provided by performing a hydrogen mass balance (or mole balance) as follows.

$$\left\{\begin{matrix}\text{moles of hydrogen}\\ \text{accumulated}\end{matrix}\right\} = \left\{\begin{matrix}\text{moles of hydrogen}\\ \text{generated}\end{matrix}\right\} + \left\{\begin{matrix}\text{moles of}\\ \text{hydrogen in}\end{matrix}\right\} - \left\{\begin{matrix}\text{moles of}\\ \text{hydrogen out}\end{matrix}\right\}$$

The system of equations capturing hydrogen transport from the Model 9979 packaging system is derived in the following subsections.

Mass Balance on the Inner Can (Layer 1)

A mass balance around the void volume of the inner can provides the following equation.

$$V_1 \frac{dC_{H_2,1}}{dt} = \eta \dot{g}_{H_2} + 0 - D_{eff,1}(y_1 - y_2) - Q_{SnO_2}\left(\sqrt{y_1} - \sqrt{y_2}\right) \quad (17)$$

The production rate of hydrogen is assumed proportional to the alpha particle production rate within the can, which is dependent on the isotope of uranium present. Hydrogen production rates for isotopes of uranium are shown in Table 4 based on an abundance of water and without the presence of back reactions that could reduce these rates. Provision is made for the hydrogen production efficiency (η) to be less than unity, as not all alpha particles will encounter a water molecule prior to absorption and thermalization and not all water encounters will produce hydrogen gas. Specific production rates are provided below.

Table 4. Hydrogen production based on mass of uranium isotope inside the inner can when water is in ample supply for all time.

Isotope	Specific hydrogen production rate[7] (moles/day/gram)
U-234	2.56×10^{-6}
U-235	8.22×10^{-10}
U-238	1.23×10^{-10}

The total moles of all gases in any layer volume is defined by the ideal gas equation.

$$n_{Tot,i} = \frac{PV_i}{RT} \quad (18)$$

Eq. (17) can be converted to mole fraction form by dividing both sides by the total moles of gas in Layer 1.

$$\frac{dy_1}{dt} = \frac{\eta \dot{g}_{H_2}}{n_{Tot,1}} - \frac{D_{eff,1}}{n_{Tot,1}}(y_1 - y_2) - \frac{Q_{SnO_2,1}}{n_{Tot,1}}\left(\sqrt{y_1} - \sqrt{y_2}\right) \quad (19)$$

Where

$$y_1 = V_1 \frac{C_{H_2,1}}{n_{Tot,1}} = \frac{C_{H_2,1}}{P/RT} \quad (20)$$

and

$$Q_{SnO_2,1} = \phi_{SnO_2,1}\sqrt{P}\left(\frac{A_1}{L_{SnO_2}}\right). \quad (21)$$

[7] Assuming the alpha decay energy is used for hydrogen production with an abundance of water molecules.

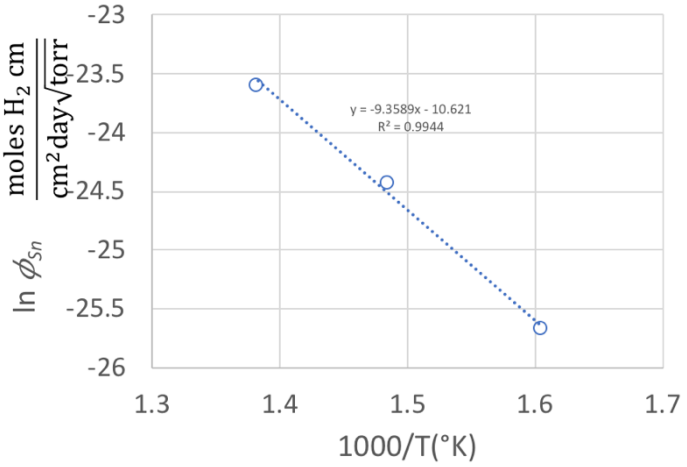

Figure 6. Hydrogen permeability through tin oxide as a function of temperature. Symbols represent data points taken from reference 8.

Hydrogen permeability through tin oxide $\left(\phi_{SnO_2}\right)$ has been reported by Bowker and Piercy[8], and is plotted in Figure 6 as a function of temperature. The temperature dependence is obtained from the fitting in Figure 6 and included in the following form.

$$\phi_{SnO_2,1} = 2.44 \times 10^{-5} \ exp^{\left(\frac{-9358.9}{T}\right)} \tag{22}$$

The transport of hydrogen through a 0.8 micron thick tin oxide layer in a 15 cm diameter can of height of 12.2 cm was calculated when the hydrogen mole fraction varied between 10^{-3} and 1 over the temperature range shown in Table 3. Hydrogen transport through the taped and crimped seams in the slip lid can was calculated at the same conditions, and was always at least 10^4 times greater than transport through the tin oxide coating. Therefore, hydrogen transport through the sides of the can was dropped from Eq. 19 such that the hydrogen mass balance in layer 1 is simplified to the following.

$$\frac{dy_1}{dt} = \frac{\eta \dot{g}_{H_2}}{n_{Tot,1}} - \frac{D_{eff,1}}{n_{Tot,1}}(y_1 - y_2) \tag{23}$$

Mass Balance on the Horsetail Bag (Layer 2)

A hydrogen gas mass balance on the horsetail bag void volume provides the following equation.

[8] Bowker, J., and G. R. Piercy, *The Effect of a Tin Barrier Layer on the Permeability of Hydrogen through Mild Steel and Ferretic Stainless Steel*, Metallurgical Transactions A 15A (1984) 2093-2095.

$$\frac{dy_2}{dt} = \frac{D_{eff,1}}{n_{Tot,2}}(y_1 - y_2) - \frac{D_{eff,2}}{n_{Tot,2}}(y_2 - y_3) \tag{24}$$

The effective diffusion coefficient of the horsetail bag $\left(D_{eff,2}\right)$ was measured at 22.85°C by Callis et al[9]. The temperature dependency was adjusted using the temperature dependence shown in Eq. 15 with the available reference temperature.

$$D_{eff,2}\big|_T = \frac{(T^{0.5}/\Omega_D)|_T}{(T^{0.5}/\Omega_D)|_{22.85°C}} D_{eff,H_2}\big|_{22.85°C} \tag{25}$$

At 22.85°C, the value of $(T^{0.5}/\Omega_D)$ for hydrogen is 19.78. Temperature dependence can also be determined in the form of Eq. 16, by plotting the calculated effective diffusivity versus the inverse temperature, as shown in Figure 7.

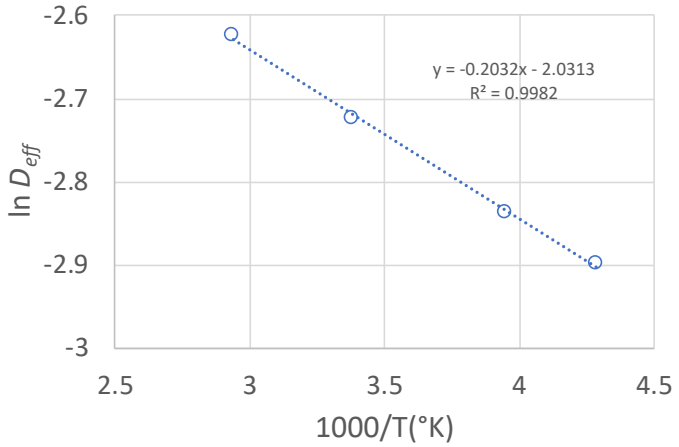

Figure 7. The effective diffusivity of the horsetail bag as a function of temperature. Calculated values over the relevant temperature range are shown as symbols.

This leads to the following familiar form.

$$D_{eff,2} = 0.131\ exp^{\left(\frac{-203.2}{T}\right)} \tag{26}$$

A comparison of Eq. 16 and 26 indicates the hydrogen diffusion from the horsetail bag is 16 times higher than from a 15 cm taped convenience can.

Mass Balance on the Outer Can (Layer 3)

A hydrogen gas mass balance on the outer can void volume provides a similar equation to Layer 2, where the effective diffusivity of the outer can follows from Equation 16.

[9] Callis, E. L., J. H. Cappis, M. C. Smith, and R. S. Marshall, *Hydrogen Venting Characteristics of Commercial Carbon-Composite Filters and Applications to TRU Waste*, LA-13284, April 1997.

$$\frac{dy_3}{dt} = \frac{D_{eff,2}}{n_{Tot,3}}(y_2 - y_3) - \frac{D_{eff,3}}{n_{Tot,3}}(y_3 - y_4) \quad (27)$$

$$D_{eff,3} = 8.15 \times 10^{-3} \left(\frac{d_3}{15\ \text{cm}}\right) exp^{\left(\frac{-203.2}{T}\right)} \quad (28)$$

Mass Balance on the 30 Gallon Drum (Layer 4)

The approach taken for hydrogen transport from the 30 gallon drum was described previously[10,11]. A hydrogen mass balance on the 30 gallon drum void volume provides the following equation.

$$\frac{dy_4}{dt} = \frac{D_{eff,3}}{n_{Tot,4}}(y_3 - y_4) - \frac{Q_{eff,4}}{n_{Tot,4}} \quad (29)$$

Where

$$Q_{eff,4} = Q_{Si} + Q_{Steel30} \quad (30)$$

$$Q_{Si} = K_{0,Si}\left(\frac{A_{Si}}{L_{Si}}\right) exp^{[0.02254(T-273.15)]} P(y_4 - y_5) \quad (31)$$

$$K_{0,Si} = \left(\frac{2.805 \times 10^{-6}\ \text{cc}_{\text{STP}}\text{cm}}{\text{cm}^2\ \text{sec atm}}\right)\left(\frac{760\ \text{torr}}{R\ 273.15°\text{K}}\right)\left(\frac{\text{atm}}{760\ \text{torr}}\right)\left(\frac{3600\ \text{sec}}{\text{hour}}\right)\left(\frac{24\ \text{hours}}{\text{day}}\right) \quad (32)$$

$$A_{Si} = \pi d_4 h_{Si} \quad (33)$$

$$Q_{Steel30} = DS_4\left(\frac{A_{4,18}}{L_{18}} + \frac{A_{4,16}}{L_{16}}\right) \quad (34)$$

$$D = 1.6 \times 10^{-3}\ \frac{\text{cm}^2}{\text{sec}}\left(\frac{3600\ \text{sec}}{\text{hour}}\right)\left(\frac{24\ \text{hours}}{\text{day}}\right) exp^{\left(\frac{-1690}{1.987T}\right)} \quad (35)$$

and

$$S_4 = S_0\sqrt{P}\left(\sqrt{y_4} - \sqrt{y_5}\right) exp^{\left(\frac{-6840}{1.987T}\right)} \quad (36)$$

[10] Blanton, P., *Hydrogen Gas Generated from the Contents in the 9979 Package*, M-CLC-A-00631, July 26, 2018.
[11] Blanton, P., Excel spreadsheet file (H2_Calculations_LANL.xlsx), created December 3, 2018.

$$S_0 = \frac{2.98\ \text{cc}_{\text{STP}}}{\text{cc}\sqrt{\text{atm}}}\left(\frac{760\ \text{torr}}{R\ 273.15°\text{K}}\right)\sqrt{\frac{\text{atm}}{760\ \text{torr}}} \tag{37}$$

$$A_{4,18} = \pi d_4 h_4 + \frac{\pi d_4^2}{4} \tag{38}$$

$$A_{4,16} = \frac{\pi d_4^2}{4} \tag{39}$$

The values of the drum diameter (d_4), height (h_4), and steel thicknesses (L_{16} and L_{18}) are provided in Table 5.

Table 5. Parameter values used in the model to represent the 30 gallon drum (Layer 4). Values were converted to the units indicated in the nomenclature prior to running simulations.

Parameter	Value
d_4 (inches)	18.25
h_4 (inches)	27.5
L_{16} (inches)	0.0598
L_{18} (inches)	0.0478

Mass Balance on the 55 Gallon Drum (Layer 5)

Assuming the 55 gallon drum is stored in an environment without hydrogen gas, a hydrogen gas mass balance on the 55 gallon drum void provides[10,11] the following equation.

$$\frac{dy_5}{dt} = \frac{Q_{eff,4} - Q_{eff,5}}{n_{Tot,5}} \tag{40}$$

where

$$Q_{eff,5} = Q_{EPDM} + Q_{Comp} \tag{41}$$

$$Q_{EPDM} = K_{0,EPDM}\left(\frac{A_{EPDM}}{L_{EPDM}}\right) exp^{[0.02331(T-273.15)]} P y_5 \tag{42}$$

$$K_{0,EPDM} = \left(\frac{2.056 \times 10^{-7}\ \mathrm{cc_{STP}cm}}{\mathrm{cm^2\ sec\ atm}}\right)\left(\frac{760\ \mathrm{torr}}{R\ 273.15°\mathrm{K}}\right)\left(\frac{\mathrm{atm}}{760\ \mathrm{torr}}\right)\left(\frac{3600\ \mathrm{sec}}{\mathrm{hour}}\right)\left(\frac{24\ \mathrm{hours}}{\mathrm{day}}\right) \quad (43)$$

$$A_{EPDM} = \pi d_{EPDM} h_{EPDM} \quad (44)$$

$$Q_{Comp} = 1/\left(\frac{2}{Q_{Steel55}} + \frac{1}{Q_{PU}}\right) \quad (45)$$

$$Q_{Steel55} = DS_5\left(\frac{A_{5,16}}{L_{16}}\right) \quad (46)$$

$$S_5 = S_0\sqrt{Py_5}\ exp^{\left(\frac{-6840}{1.987T}\right)} \quad (47)$$

$$A_{5,16} = \pi d_5 h_5 + 2\left(\frac{\pi d_5^2}{4}\right) \quad (48)$$

$$Q_{PU} = K_{0,PU}\left(\frac{A_{PU}}{L_{PU}}\right)\ exp^{[0.03825(T-273.15)]} Py_5 \quad (49)$$

$$K_{0,PU} = \left(\frac{4.639 \times 10^{-8}\ \mathrm{cc_{STP}cm}}{\mathrm{cm^2\ sec\ atm}}\right)\left(\frac{760\ \mathrm{torr}}{R\ 273.15°\mathrm{K}}\right)\left(\frac{\mathrm{atm}}{760\ \mathrm{torr}}\right)\left(\frac{3600\ \mathrm{sec}}{\mathrm{hour}}\right)\left(\frac{24\ \mathrm{hours}}{\mathrm{day}}\right) \quad (50)$$

and

$$A_{PU} = A_{5,16}\ . \quad (51)$$

Parameters used in the description of 55 gallon drum (Layer 5) are provided in Table 6.

Table 6. Parameter values used in the model to represent the 55 gallon drum (Layer 5). Values were converted to the units indicated in the Nomenclature section prior to running simulations.

Parameter	Value
d_{EPDM} (inches)	22.5
h_{EPDM} (inches)	0.25
L_{EPDM} (inches)	1
d_5 (inches)	19.75
h_5 (inches)	30
L_{16} (inches)	0.0598

Dynamic Model and Solution Method

The time-dependent system of equations is defined by Eq. 23, 24, 27, 29, and 40, which are listed below for convenience.

$$\frac{dy_1}{dt} = \frac{\eta \dot{g}_{H_2}}{n_{Tot,1}} - \frac{D_{eff,1}}{n_{Tot,1}}(y_1 - y_2)$$

$$\frac{dy_2}{dt} = \frac{D_{eff,1}}{n_{Tot,2}}(y_1 - y_2) - \frac{D_{eff,2}}{n_{Tot,2}}(y_2 - y_3)$$

$$\frac{dy_3}{dt} = \frac{D_{eff,2}}{n_{Tot,3}}(y_2 - y_3) - \frac{D_{eff,3}}{n_{Tot,3}}(y_3 - y_4)$$

$$\frac{dy_4}{dt} = \frac{D_{eff,3}}{n_{Tot,4}}(y_3 - y_4) - \frac{Q_{eff,4}}{n_{Tot,4}}$$

$$\frac{dy_5}{dt} = \frac{Q_{eff,4} - Q_{eff,5}}{n_{Tot,5}}$$

A MATLAB script was written to integrate the dynamic model equations. The nonstiff differential equation solver *ODE45* was applied with an absolute tolerance of 10^{-12}, a relative tolerance of 10^{-9}, and nonnegative values declared for all mole fractions. Integration over a 1200 day period is shown in Figure 8. Hydrogen concentration is shown to be highest in layer 1 and decreasing in each subsequent layer down to layer 5. All simulations followed this order.

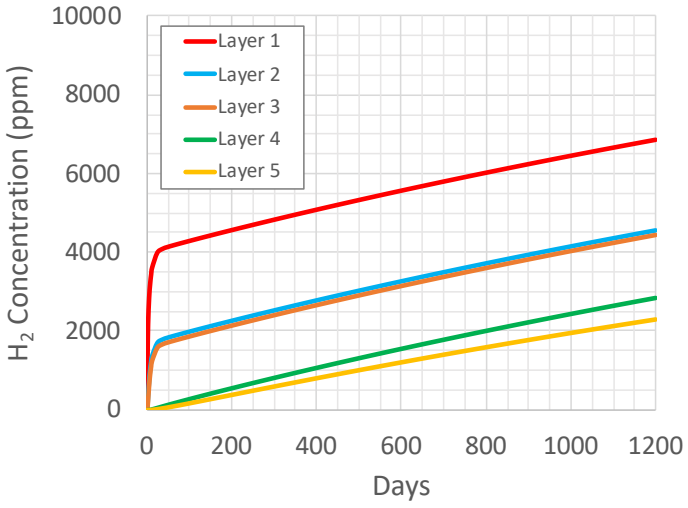

Figure 8. Dynamic concentration profiles of the 5 layer model over a 1200 day period. See Table 10 (storage) for model parameters used.

Steady-State Model and Solution Method

The steady-state form of the model is obtained by setting the accumulation term to zero, which generates the following set of algebraic equations.

$$\eta \dot{g}_{H_2} = D_{eff,1}(y_1 - y_2) \tag{52}$$

$$D_{eff,1}(y_1 - y_2) = D_{eff,2}(y_2 - y_3) \tag{53}$$

$$D_{eff,2}(y_2 - y_3) = D_{eff,3}(y_3 - y_4) \tag{54}$$

$$D_{eff,3}(y_3 - y_4) = Q_{eff,4} \tag{55}$$

$$Q_{eff,4} = Q_{eff,5} \tag{56}$$

There are two notable characteristics of the steady-state equations. Firstly, as the accumulation term is the source of $n_{Tot,i}$ in the dynamic model equations, the steady-state solution does not depend on any specific void volume. Secondly, the hydrogen generation rate given by the left hand side of Eq. 52 can be set equal to the right hand side of each subsequent equation. This later feature leads to a convenient method to obtain the steady state solution. The steady state solution of y_5 is solved first in the sequence by setting the hydrogen generation rate to $Q_{eff,5}$ (i.e., the right hand side of Eq. 56). Working in reverse order, the same approach can be used to solve Eq. 55 through 52 for y_4 through y_1, respectively. This method was followed using Microsoft Excel's *Solver* tool to verify the accuracy of the solutions obtained by the dynamic model at long times (i.e., around 100,000 days). Imposing a precision of 10^{-10}, the steady-state hydrogen concentrations were within 1 ppm of the dynamic model for all long time simulations.

Resistance to Transport Based on Model Parameter Values

Model parameters calculated at the average atmospheric pressure in Los Alamos (582 torr) and at transport and storage temperatures are provided in Table 7. Convenience can sizes and layer volumes are as shown in Table 10. The ratio of the mass transfer parameters to total moles indicates the rate of transport across a given barrier. The convenience cans and horsetail bag facilitate hydrogen transport more so than either the 30 or 55 gallon drum, and the horsetail bag offers an order of magnitude higher rate than the convenience cans. The hydrogen concentration change across any given barrier is indicated by the ratio of $\dot{g}_{H_2}$ to the transport parameter (D or Q). At steady-state, the change in hydrogen concentration across the horsetail bag is expected to be lower than across either inner or outer convenience can, and the change in hydrogen concentration across the 55 gallon drum is expected to be higher than the change across any of the convenience cans.

Table 7. Calculated model parameters at shipping and storage temperatures.

Parameter	Temperature (°C)		
	-40	-28.89	20
$n_{Tot,1}$	4.80×10^{-3}	4.58×10^{-3}	3.82×10^{-3}
$n_{Tot,2}$	4.00×10^{-4}	3.82×10^{-4}	3.18×10^{-4}
$n_{Tot,3}$	4.00×10^{-2}	3.82×10^{-2}	3.18×10^{-2}
$n_{Tot,4}$	2.39	2.28	1.90
$n_{Tot,5}$	1.57	1.50	1.25
$\dot{g}_{H_2}$	$\leq 8.26 \times 10^{-6}$	$\leq 8.26 \times 10^{-6}$	$\leq 8.26 \times 10^{-6}$
$D_{eff,1}$	3.00×10^{-3}	3.12×10^{-3}	3.59×10^{-3}
$D_{eff,2}$	5.48×10^{-2}	5.70×10^{-2}	6.55×10^{-2}
$D_{eff,3}$	4.32×10^{-3}	4.49×10^{-3}	5.16×10^{-3}
$Q_{Si}/(y_4 - y_5)$	1.28×10^{-4}	1.64×10^{-4}	4.95×10^{-4}
$Q_{Steel30}/(\sqrt{y_4} - \sqrt{y_5})$	1.76×10^{-5}	4.08×10^{-5}	7.64×10^{-4}
Q_{EPDM}/y_5	1.07×10^{-5}	1.39×10^{-5}	4.34×10^{-5}
$Q_{Steel55}/\sqrt{y_5}$	1.49×10^{-5}	3.45×10^{-5}	6.47×10^{-4}
Q_{PU}/y_5	1.19×10^{-4}	1.82×10^{-4}	1.18×10^{-3}

Summary of Model Assumptions

The assumptions employed to formulate the system of equations are listed below.

- The model 9979 package and can assembly is as shown in Figure 1, with all radioactive material in a single inner can.
- The inner can does not contain organic material such as paper or plastic that could serve as a second source of hydrogen.
- Water in a condensed form and as a vapor is available in unlimited quantities in the inner can, and as a vapor is pervious to all layers in the 9979 package. This assumption is relaxed when an efficiency factor less than 1 is employed in the calculations.
- Hydrogen removal by back reaction with free radicals formed by alpha particle induced excitation and ionization is not considered.
- All gases obey the ideal gas law.

- Transport of gases from the inner and outer cans occurs as a consequence of steady-state equimolar (isobaric) counterdiffusion.
- The area perpendicular to the molar flux through the taped gap and crimped seams of the inner and outer cans is proportional to the circumference of the can, and hence the can diameter.
- Transport of gases from the horsetail bag occurs as a consequence of steady-state equimolar (isobaric) counterdiffusion.
- Transport of gases from the 30 gallon drum and 55 gallon drum are as described previously by Blanton[10,11].
- The 9979 package is stored in a location where the hydrogen gas mole fraction is zero.

Model Simulations

The model as presented was used to calculate hydrogen accumulations for two purposes; (i) to check model predictions against measured values, and (ii) to look specifically at each layer's hydrogen concentration as a package over its lifetime. A model check was performed by simulating the storage of packages at LANL's Chemistry and Metallurgy Research (CMR) building, and comparing them to actual measurements taken after approximately 500 days. Lifetime assessments were performed by simulating the storage, transportation, and disposal of packages at different transportation and disposal conditions. The results are described below.

Five 9979 Packages Stored for around 500 Days

The CMR uses the DOE approved Model 9979 Type AF shipping package shown in Figure 1 to stage and ship fissile uranium metals, oxides and other solid compounds to off-site disposal facilities[12]. This device does not permit continuous venting under normal conditions of staging or transport, and recent communication with DOE suggests 30 gallon drums (layer 4) that have not been vented in 6 months may potentially generate hydrogen gas as a result of radioactive decay and the presence of hydrogen-bearing material. CMR has approximately 68 of the 9979 Type AF containers (packaged in 2016 and 2017), with the majority of these having Highly Enriched Uranium (HEU) content as defined in S-SARP-G-00006, R4, (SARP)[13]. These containers, categorized as LLW, will ultimately be shipped to the NNSS for disposal. As required in CIIAC-CMR-IWD-002, detailed documentation regarding the contents of each container was collected during packaging operations. Based on this information, five containers were chosen for hydrogen monitoring based on the following criteria:

- Maximum potential wattage (i.e., mass of uranium material).
- Maximum ratio of hydrogenous material (i.e., outside of the inner can) to uranium.

[12] French, S. B., *Hydrogen Gas Concentration in Model 9979 Type AF Containers at Los Alamos National Laboratory*, LA-UR-18-29921, (Rev. 0) October 2018.

[13] S-SARP-G-00006, R4, *Safety Analysis Report for Packagings: Model 9979 Type AF Shipping Package,* S-SARP-G-00006 (Rev. 4), Savannah River National Laboratory, March 2015.

- Maximum volume of the inner containers packed into each 30 gallon drum which minimizes the air volume available for hydrogen.

These five containers were also used as a check for the hydrogen transport model calculations. Table 8 lists known parameters for the five containers, while the remaining model parameters had to be assumed. Values used for the assumed parameters are provided in Table 9.

Table 8. Description of the 5 packages selected for monitoring.

Order for Monitoring	**Drum Number**	Maximum $\dot{g}_{H_2}$ **(moles/day)**	V_4 **(cm³)**	**Day Sampled**	**Measured** $[H_2]$ **(ppm)**	**Description**
1	4024Drum#36	9×10^{-8}	88,400	498	9.2 ± 1.4	Compound Fluoride
2	4040Drum#3	1×10^{-5}	88,400	520	3 ± 0.5	Process Residue Salt
3	4033Drum#16	2.9×10^{-6}	88,400	541	540 ± 80	Process Residue Salt
4	4033Drum#14	3.9×10^{-6}	74,000	553	97 ± 15	Metal Unalloyed
5	4033Drum#12	7.8×10^{-6}	59,700	553	62 ± 9	Process Residue Salt

Table 9. Model parameter values assumed.

Parameter	**Value**
P (torr)	582
T (°C)	20
η	1
d_1 (cm)	13.2
V_1 (cm³)	120[14]
V_2 (cm³)	10[15]
d_3 (cm)	19
V_3 (cm³)	1,000[16]
V_4 (cm³)	See values in Table 8
V_5 (cm³)	39,200[17]

[14] Discussions with L. Ortega on 13 November 2018 indicated an approximate void volume ranging between 10 and 70% of the can volume. Minimum void volume of 10% of the can volume was assumed.

[15] Void volume estimated based on a tightly wrapped can.

[16] Minimum void volume of all 1st and 3rd layer can combinations.

[17] Void volume taken from Blanton (reference 11).

Hydrogen concentrations were calculated using the hydrogen transport model at the sampling time listed in Table 8 for each of the five packages. The model calculations are compared to the measured values in Figure 9, which leads to the following conclusions:

- Hydrogen gas concentrations calculated in the 30 gallon container (layer 4) are shown to bound the measured values in 4 of the 5 drums. The uncertainty of the hydrogen concentration measurements is ±15%. The hydrogen concentration in the one outlier package (i.e., 4033Drum#16) is about 48% higher than the predicted value, and likely results from organic material in the inner can as evinced by the detection of methane[18].
- Uncertainty of the hydrogen transport model has not been assessed. A sensitivity analysis was performed on the model parameters around the assumed values, and it was concluded the only parameter that could account for the dramatically low hydrogen content in 3 of the 5 packages is the hydrogen generation rate efficiency factor. This reinforces the concept of applying $\eta = 1$ for a conservative estimate of hydrogen distribution in the 9979 package. Deviation between the calculated and measured values for the remaining two packages can be accommodated by uncertainties in other model parameters. A 10% reduction in layer 4 void volume increases the hydrogen concentration by around 7%. Increasing the effective diffusivity of hydrogen to that measured in Can 2 increases the hydrogen concentrations in layer 4 by only 1 to 2 ppm.
- Comparison to measured hydrogen concentrations in the 5 drums suggests the assumed values of the model parameters listed in Table 9 are reasonable for the purpose of calculating maximum hydrogen gas buildup in the 9979 package to within 50%.
- Hydrogen content calculated for the inner container in all 5 packages is well below the LFL value of 40,000 ppm.

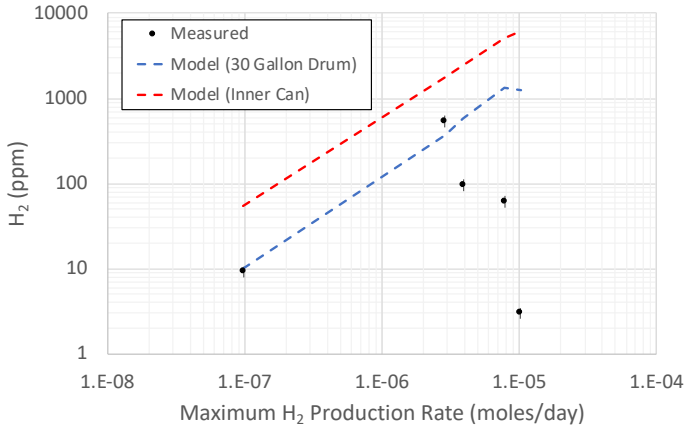

Figure 9. Hydrogen concentration measured in 5 packages around 500 days following packaging. Measured values (i.e., the black data points with ± 15% uncertainty) are compared to concentrations calculated by the hydrogen transport model. Calculated hydrogen concentrations in the 30 gallon container (blue line) are shown to bound the measured values in 4 cases, which are well below the values calculated for the inside can (red line). The LFL is out of range on the plot at 40,000 ppm.

[18] 12 ppm methane was detected in the 30 gallon head space in 4033DRUM#16.

The bounding predictions provided by the hydrogen transport model provide a suitable context for considering hydrogen accumulation in various lifetime scenarios.

Package Storage, Transport, and Disposal Simulation

The lifetime conditions of any given package will be unique as a consequence of the amount of radioactive materials contained as well as its thermal and site history. To simplify the number of scenarios simulated, extreme conditions are considered for the sake of identifying worst case hydrogen accumulation in the inner can. These conditions are described below.

- *Radioactive material corresponding to the LANL Criticality Limit.* The LANL Criticality Limit is met by a container with 1.5 g of U-234, 200 g of U-235, and 4900 g of U-238, and corresponds to a hydrogen production rate of 4.61×10^{-6} moles per day.
- *Radioactive material corresponding to the LANL Packaging Limit.* The LANL Packaging Limit is met by a container with 2.7 g of U-234, 350 g of U-235, and 8647.3 g of U-238, and corresponds to a hydrogen production rate of 8.26×10^{-6} moles per day.
- *Maximum storage time.* Model 9979 containers are assumed to be stored at LANL for a maximum period of 1200 days. Containers are stored at the CMR, which is kept at room temperature (20°C).
- *Extremely cold transportation temperatures.* Transportation at cold wintertime conditions results in the highest hydrogen accumulation rate in the innermost can. Arctic air incursions into the continental U.S. can persist for several days, sometimes bringing winter storms and highway closures. Therefore, a 14 day transportation period is considered at two temperature extremes; -28.89°C (-20°F) and -40°C (-40°F).
- *Disposal of the 9979 package by burial at the Nevada Test Site for eternity.* Long time simulation captures the equilibrium hydrogen concentration in the inner can. Three temperatures of interest at Beatty, NV[19] are considered; the average high temperature (23.4°C), the average temperature (14.75°C), the average low temperature (6.1°C).
- *Neglecting hydrogen dilution at transition points leads to conservative estimates of hydrogen concentration in the inner can.* The internal pressure of the 9979 package changes with temperature and atmospheric pressure, and the effect on hydrogen concentration was not accounted for in these simulations. Pressure inside the 9979 package becomes higher than atmospheric in all but one condition when transitioning from transportation to burial. Increased pressure inside the package would equilibrate by convection of gas out of the package (if possible). This would not affect the hydrogen concentration in the inner can, but would slightly raise hydrogen concentrations in all other layers as they receive gas from the more concentrated adjacent layer. The total moles of gas in the 9979 package would decrease by 1 to 8.4% in these pressurization scenarios. Transitioning from -28.89°C transport to 6.1°C burial and from storage to

[19] Temperature and altitude data taken obtained from: https://www.usclimatedata.com/climate/beatty/nevada/united-states/usnv0007, accessed on 1/24/2019.

transport results in a pressure deficit which would equilibrate by convection of air into the package (if possible). This would dilute hydrogen most dramatically in the outermost layer and to a lesser extent in the inner layers as they receive gas from the less concentrated adjacent layer. Transitioning from storage to transport would increase the total moles of gas in the 9979 package between 20 and 26%, and by only 2% in the case of the highest transport temperature and lowest burial temperature. For the purpose of the simulations, a simple but conservative approach was taken. That is, continuity of hydrogen mole fractions was assumed at all transition points while temperature and pressure changes were assumed to occur instantaneously. This approach maintains the highest possible hydrogen concentrations in the innermost layer, which would be the first layer to exceed the hydrogen LFL in the 9979 package.

The hydrogen transport model was applied under these conservative conditions using the model parameters shown in Table 10. The hydrogen concentration profiles in the inner can are shown in Figure 10 and Figure 11, and suggest effects from the extreme shipping temperatures are insignificant relative to the radioactive material content and final burial temperature. For example, the hydrogen concentration in the inner can containing the LANL Packaging Limit reached 7562 ppm at -40°C and 7415 ppm at -28.89°C, a difference of around 2%. The time-dependent hydrogen concentration in the 30 gallon drum (layer 4) is shown in Figure 12, and changed by less than 50 ppm during transportation with differences of less than 5 ppm at the two temperature extremes. The dynamic model solutions were always found to be well below the hydrogen LFL, and in agreement with the steady state values at long times (i.e., around 100,000 days).

Table 10. Parameters used in the hydrogen transport model for lifetime hydrogen profile calculations.

Parameter	Storage at Los Alamos, NM	Transportation Period	Disposal at Beatty, NV
P (torr)	582	582	678
T (°C)	20	-28.89 or -40	6.1, 14.75, or 23.4
η	1		
d_1 (cm)	13.2		
V_1 (cm^3)	120[14]		
V_2 (cm^3)	10[15]		
d_3 (cm)	19		
V_3 (cm^3)	1000[16]		
V_4 (cm^3)	59,700[20]		
V_5 (cm^3)	39,200[17]		

[20] Minimum void volume listed in Table 8.

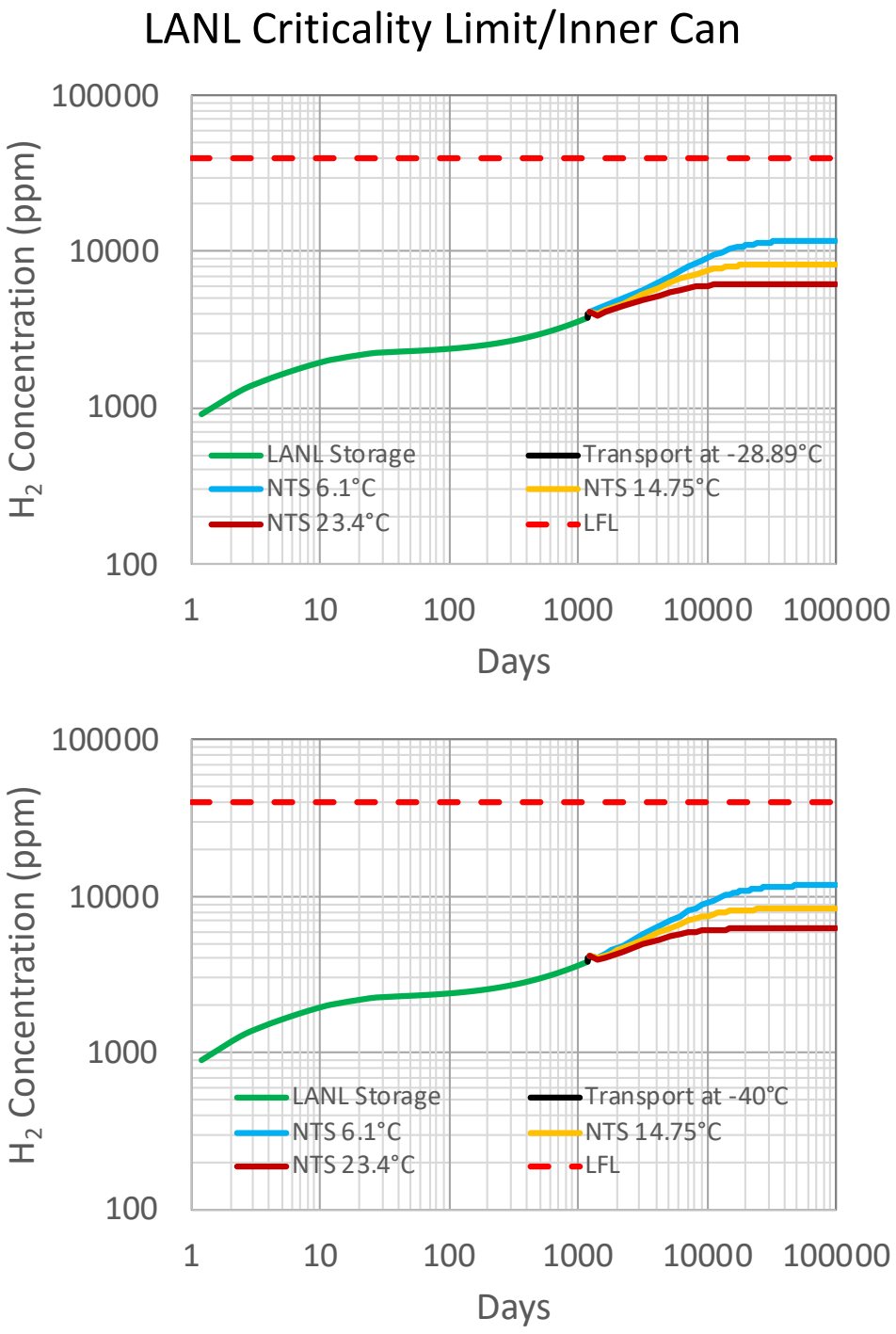

Figure 10. Dynamic calculation of hydrogen accumulation in the inner can (layer 1) containing radioactive material corresponding to the LANL Criticality Limit. The upper figure was generated using a transportation temperature of -28.89°C, while the lower figure uses -40°C.

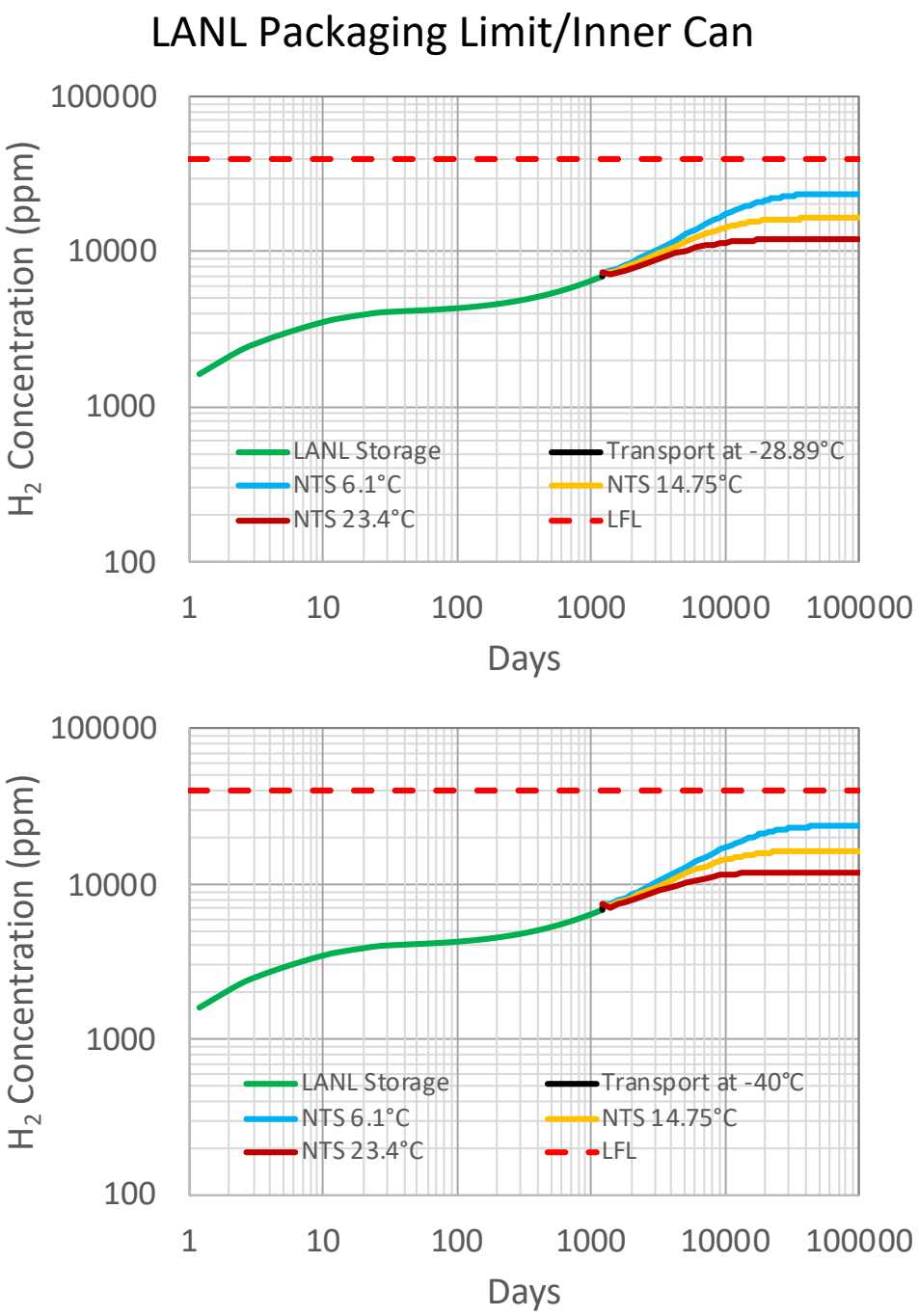

Figure 11. Dynamic calculation of hydrogen accumulation in the inner can (layer 1) containing radioactive material corresponding to the LANL Packaging Limit. The upper figure was generated using a transportation temperature of -28.89°C, while the lower figure uses -40°C.

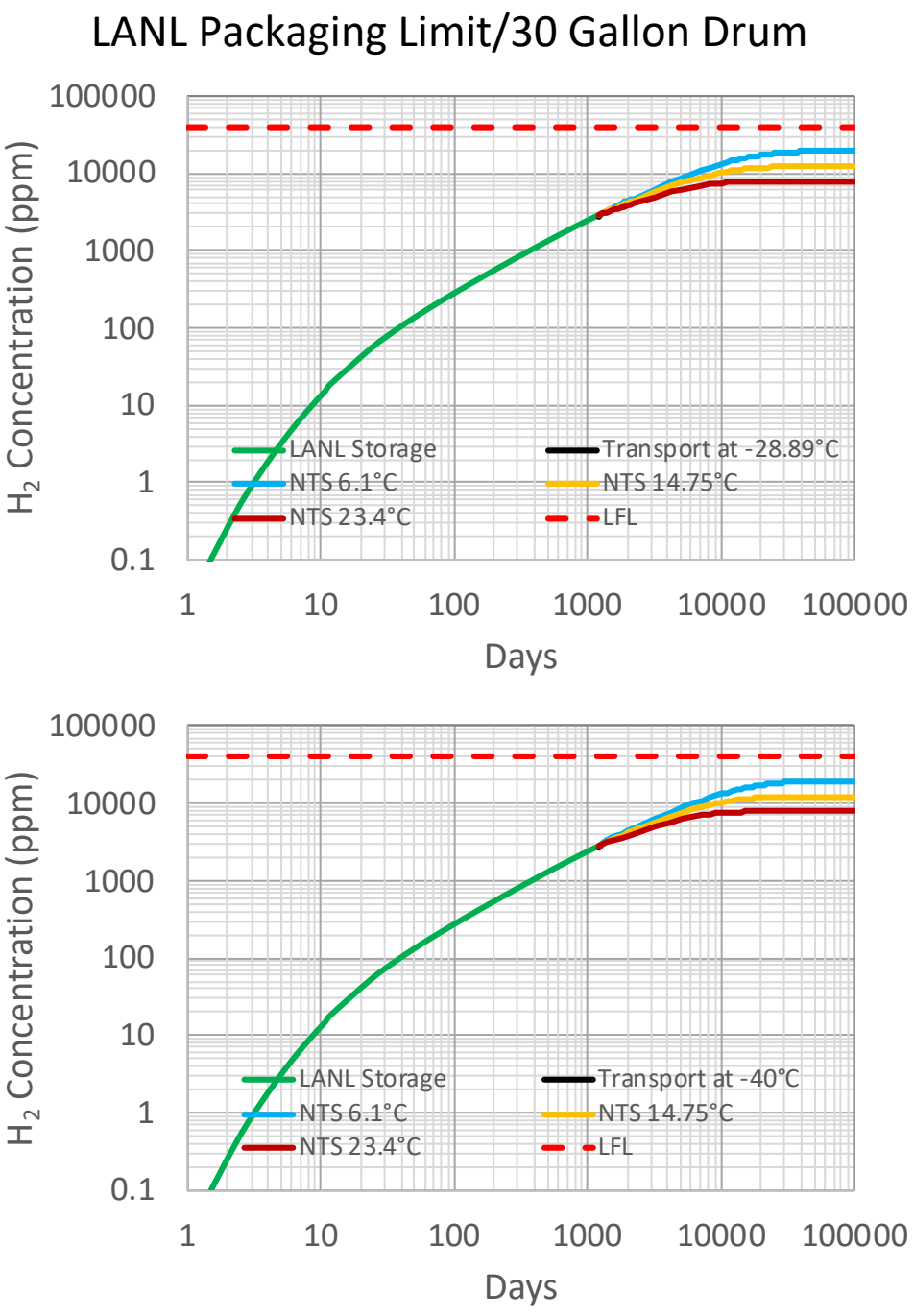

Figure 12. Dynamic calculation of hydrogen accumulation in the 30 gallon drum (layer 4) when the radioactive material in the inner can meets the LANL Packaging Limit. The upper figure was generated using a transportation temperature of -28.89°C, while the lower figure uses -40°C.

Conclusions

A hydrogen transport model is presented for a Model 9979 package system containing a nested arrangement of slip-lid convenience cans. The inner convenience can contains the radioactive source material and incidental quantities of water. It is tape sealed, wrapped in a plastic bag, and then placed into an outer convenience can. This can assembly is placed into the 30 gallon drum in the 9979 package which is subsequently placed inside a 55 gallon drum. The model was used to calculate hydrogen accumulations within these five layers for two purposes; to check model predictions against measured values, and to look specifically at a package over its lifetime. A model check was performed by simulating the storage of packages at the LANL CMR building, and comparing them to actual measurements taken after approximately 500 days of storage. Lifetime assessments were performed by simulating the storage, transportation, and disposal of packages at different transportation and disposal conditions.

Maximum hydrogen concentrations obtained from hydrogen transport model simulations were compared to measured values from 5 packages. Gas samples were collected from the 30 gallon drum layer after approximately 500 days of storage at the CMR building. Calculated hydrogen gas concentrations were shown to bound the measured values in 4 of 5 packages. The hydrogen concentration in the one outlier package (i.e., 4033Drum#16) is about 48% higher than the predicted value, and likely results from organic material in the inner can as evinced by the detection of methane. Bounding of the measured hydrogen concentrations suggests the parameter values used in the model are reasonable for the purpose of estimating maximum hydrogen gas accumulation in the 9979 package to within 50%. Hydrogen content calculated for the innermost container in all 5 packages is well below the Hydrogen LFL value. A sensitivity analysis was performed on the model parameters around the assumed values, and it was concluded the only parameter that could account for the dramatically low hydrogen content in three of the five packages is the hydrogen generation rate efficiency factor. This reinforces the concept of applying an efficiency factor of 1 for conservative estimates of hydrogen distribution in the 9979 package.

The transport model was also used to calculate maximum hydrogen concentrations in various lifetime scenarios whereby packages were subjected to extreme storage, transportation, and disposal conditions. A storage period of 1200 days was applied, which is a longer than the maximum expected. A two week transportation period was assumed at extremely cold temperatures that severely reduce the transport of hydrogen out of the package. And finally, different average temperatures were assumed for disposal of the packages. The conditions of any given package are unique as a consequence of the amount of radioactive materials contained as well as its thermal and site history. Two extreme radioactive material limits were considered for the sake of identifying credible worst case hydrogen accumulation in the inner can.

1. LANL Criticality Limit: 1.5 g of U-234, 200 g of U-235, and 4900 g of U-238.
2. LANL Packaging Limit: 2.7 g of U-234, 350 g of U-235, and 8647.3 g of U-238.

The LANL Criticality Limit contains is a very conservative limit and roughly half the radioactive material as is in the LANL Package Limit. The hydrogen concentration is always highest in the inner convenience can and was calculated over periods exceeding 270 years where steady state values are approached. Simulations consisted of the following three distinct segments.

1. **Assembly and storage.** Assembly of the 9979 package was assumed to occur at LANL's CMR building, where it is stored for 1200 days at 20°C and 582 torr.
2. **Transportation.** Following storage, the 9979 package is transported to the Nevada Test Site (NTS) over a 14 day period at one of two extreme temperature conditions; either -28.89°C (-20°F) or -40°C (-40°F). Neither temperature raised concerns with the hydrogen LFL due to the relatively short time period. Atmospheric pressure was assumed constant at 582 torr, the average for Los Alamos, NM. Atmospheric pressure would more realistically transition from 582 to 678 torr, the average atmospheric pressure for Beatty, NV. Increasing atmospheric temperature has two disproportionate counteracting effects. High pressure air would flow into the 9979 package and drive down hydrogen concentrations. At the same time, increasing package pressure would reduce hydrogen diffusivity resulting in slightly more hydrogen accumulation. Even though the dilution effect is estimated to be larger than the net gain in hydrogen due to reduced diffusivity, assuming continuity of pressure and hydrogen concentrations through the transport period simplifies the calculations and provides more conservative estimates of hydrogen concentration throughout the 9979 package.
3. **Final disposition (burial).** Burial of the 9979 package was assumed to occur at Beatty, NV, where the average atmospheric pressure is 678 torr. Three temperatures were considered for this final lifetime segment; the average low temperature of 6.1°C, the average temperature of 14.75°C, and the average high temperature of 23.4°C. While it is likely the initial hydrogen concentrations in a 9979 package would be slightly reduced following pressurization in the Beatty atmosphere, the hydrogen concentrations calculated at the end of the transportation period were taken without change as the initial values for the final disposition period. Maintaining continuity of hydrogen concentrations between the transportation and disposition segments is consistent with the desire to provide conservative estimates of hydrogen concentration in the 9979 package.

Lifetime simulations of the hydrogen concentration in the inside can indicate steady state conditions are reached after several decades and at no time encroach on the hydrogen LFL. Solutions at long times (i.e., around 100,000 days) obtained with the dynamic model were found to be in agreement with the steady state values. Therefore, this analysis shows that 9979 drums packaged at LANL will never exceed nor closely approach the hydrogen LFL needed for a deflagration or fire event. Extended storage at LANL, extremely cold transportation temperatures, or burial at Beatty, NV will not alter the safe levels of hydrogen in the container system even over extremely long times.

Acknowledgements

The authors would like to thank Loretta Ortega and Randy Walker (C-AAC) for discussions on the procedure and practices followed in assembling the inner and outer cans. J. Coons would like to thank Paul Blanton and Joshua Flach of Savannah River National Laboratory for discussions and information related to hydrogen transport through the 30 gallon and 55 gallon drums. J. Coons would also like to thank John Tanski (A-2) for discussions early on in the modeling effort and for assistance with accessing solution values at each time step in the dynamic model.